Supplementary Material of "Analysis of Partition Methods for Dominated Solution Removal from Large Solution Sets"

S1. Performance Comparison among Different Methods

Figure 1-3, Figure 4 and Figure 5 show the performance comparison of different methods in terms of the average computation time and the average number of remaining dominated solutions on the WFG, DTLZ and RE problems, respectively.

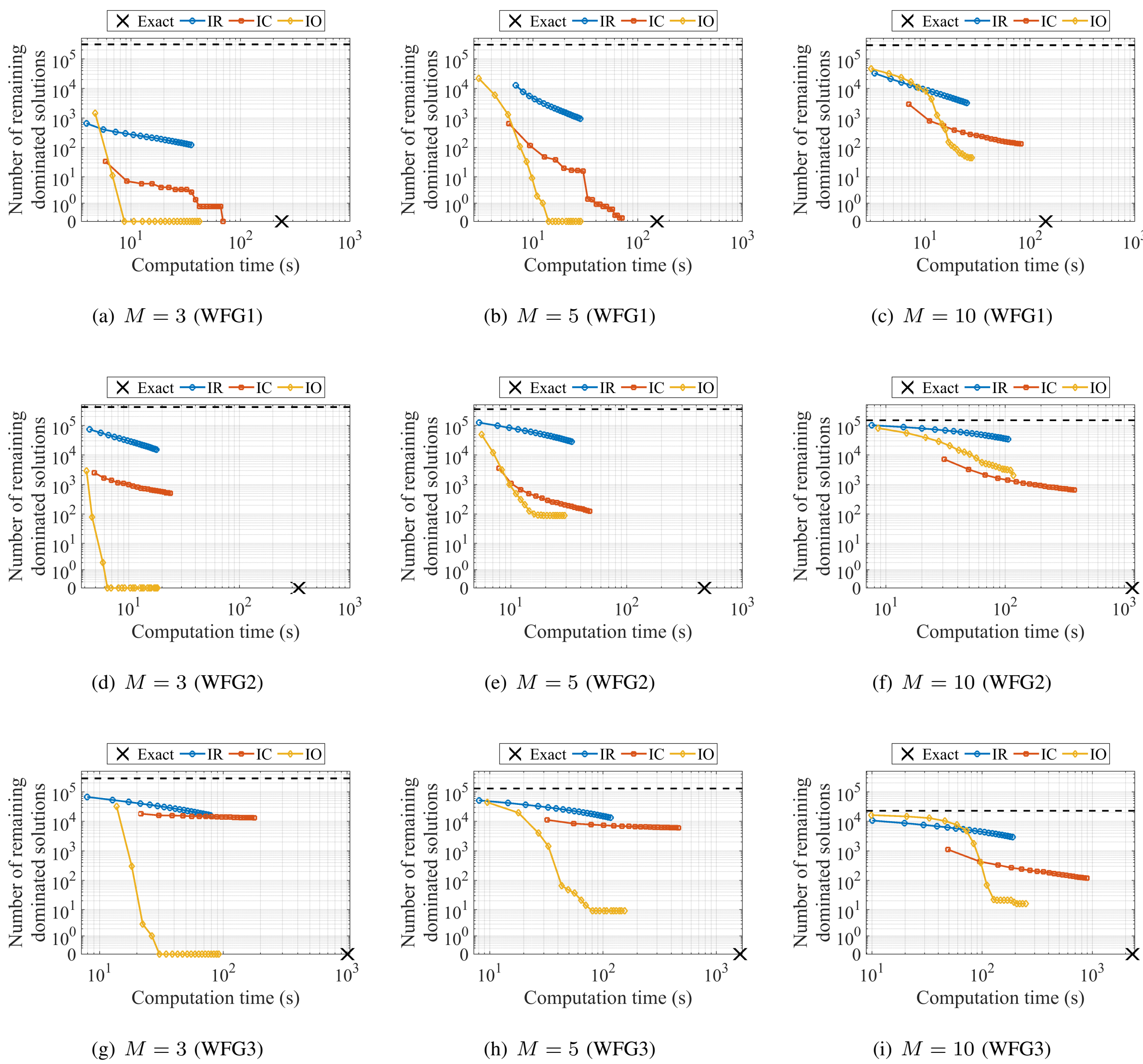

(a) $M = 3$ (WFG1) (b) $M = 5$ (WFG1) (c) $M = 10$ (WFG1)

(d) $M = 3$ (WFG2) (e) $M = 5$ (WFG2) (f) $M = 10$ (WFG2)

(g) $M = 3$ (WFG3) (h) $M = 5$ (WFG3) (i) $M = 10$ (WFG3)

Fig. 1. Performance comparison of different methods for removing dominated solutions from the WFG1-3 problems. Average values over ten runs are shown.

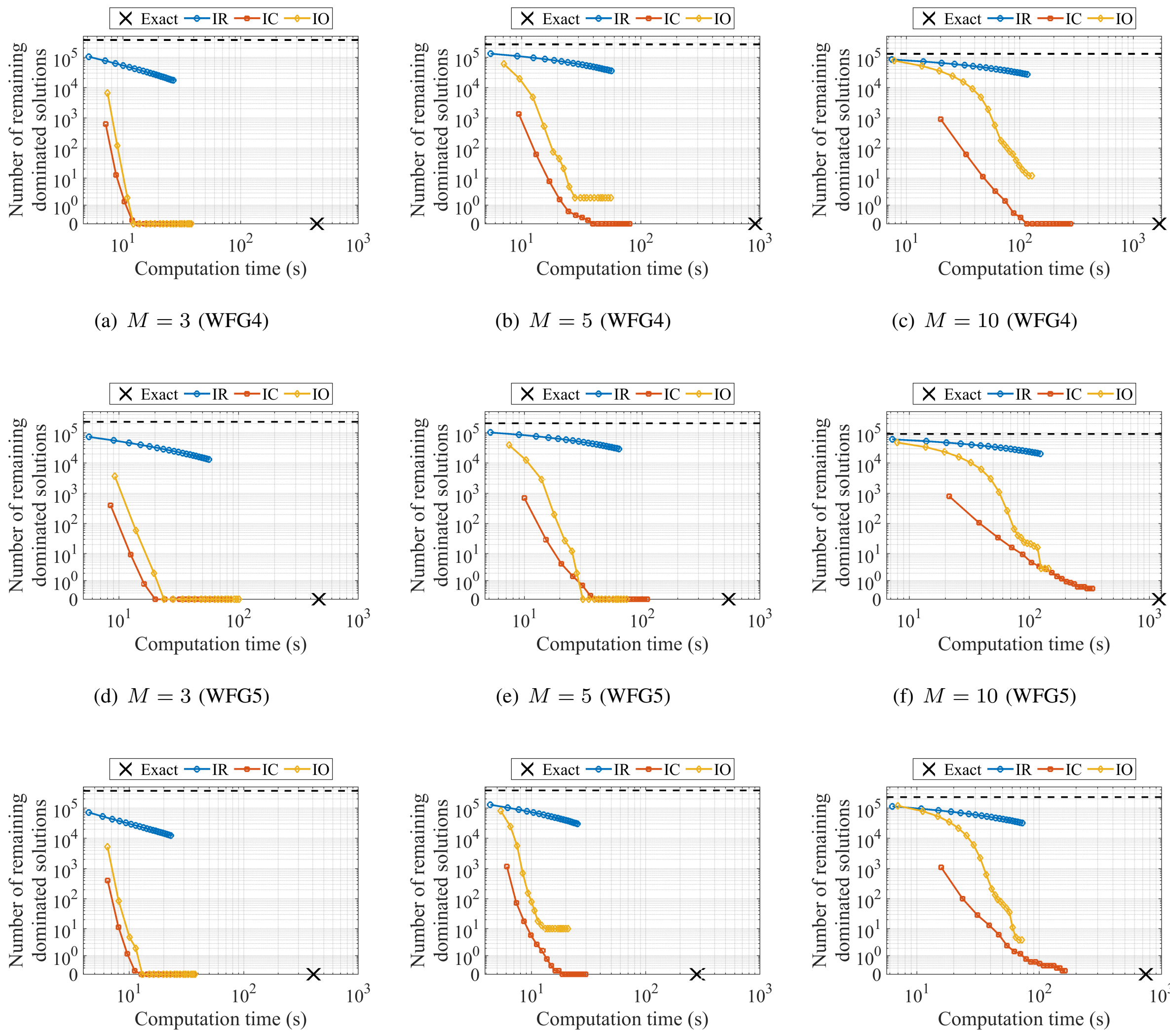

(a) $M = 3$ (WFG4) (b) $M = 5$ (WFG4) (c) $M = 10$ (WFG4)

(d) $M = 3$ (WFG5) (e) $M = 5$ (WFG5) (f) $M = 10$ (WFG5)

(g) $M = 3$ (WFG6) (h) $M = 5$ (WFG6) (i) $M = 10$ (WFG6)

Fig. 2. Performance comparison of different methods for removing dominated solutions from the WFG4-6 problems. Average values over ten runs are shown.

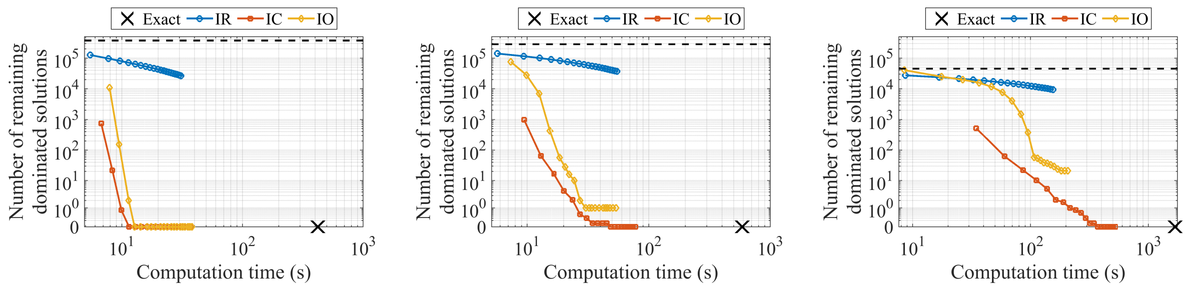

(a) $M = 3$ (WFG7) (b) $M = 5$ (WFG7) (c) $M = 10$ (WFG7)

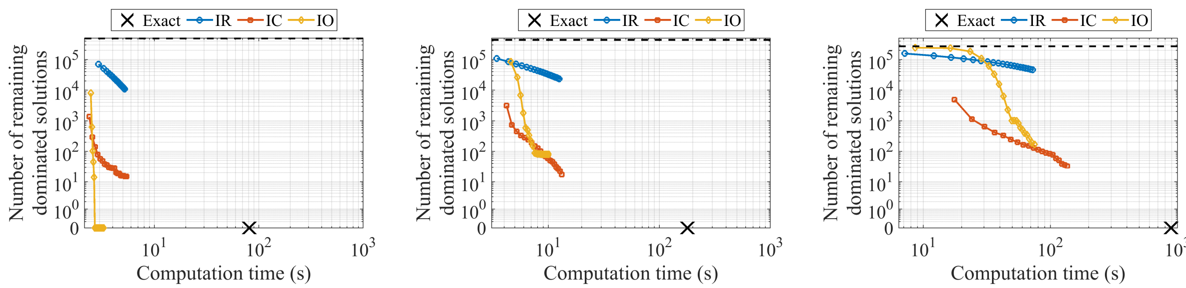

(d) $M = 3$ (WFG8) (e) $M = 5$ (WFG8) (f) $M = 10$ (WFG8)

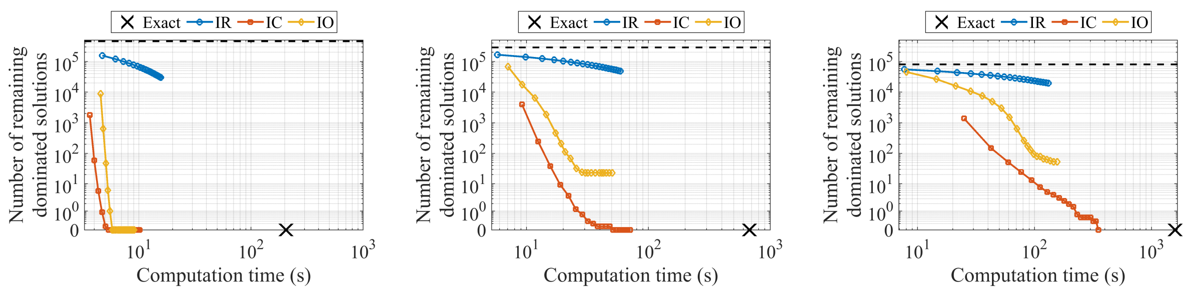

(g) $M = 3$ (WFG9) (h) $M = 5$ (WFG9) (i) $M = 10$ (WFG9)

Fig. 3. Performance comparison of different methods for removing dominated solutions from the WFG7-9 problems. Average values over ten runs are shown.

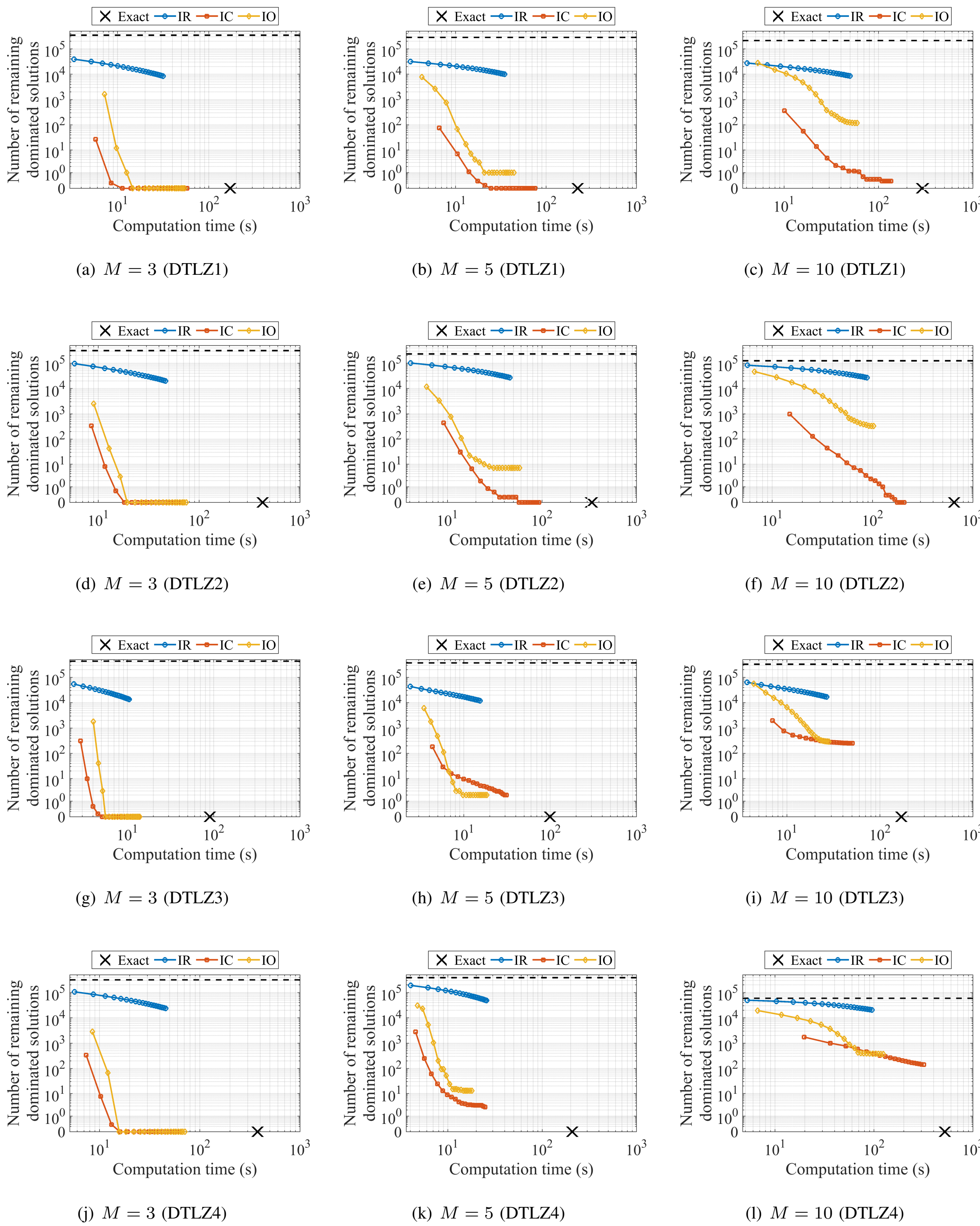

(a) $M = 3$ (DTLZ1) (b) $M = 5$ (DTLZ1) (c) $M = 10$ (DTLZ1)

(d) $M = 3$ (DTLZ2) (e) $M = 5$ (DTLZ2) (f) $M = 10$ (DTLZ2)

(g) $M = 3$ (DTLZ3) (h) $M = 5$ (DTLZ3) (i) $M = 10$ (DTLZ3)

(j) $M = 3$ (DTLZ4) (k) $M = 5$ (DTLZ4) (l) $M = 10$ (DTLZ4)

Fig. 4. Performance comparison of different methods for removing dominated solutions from the DTLZ1-4 problems. Average values over ten runs are shown.

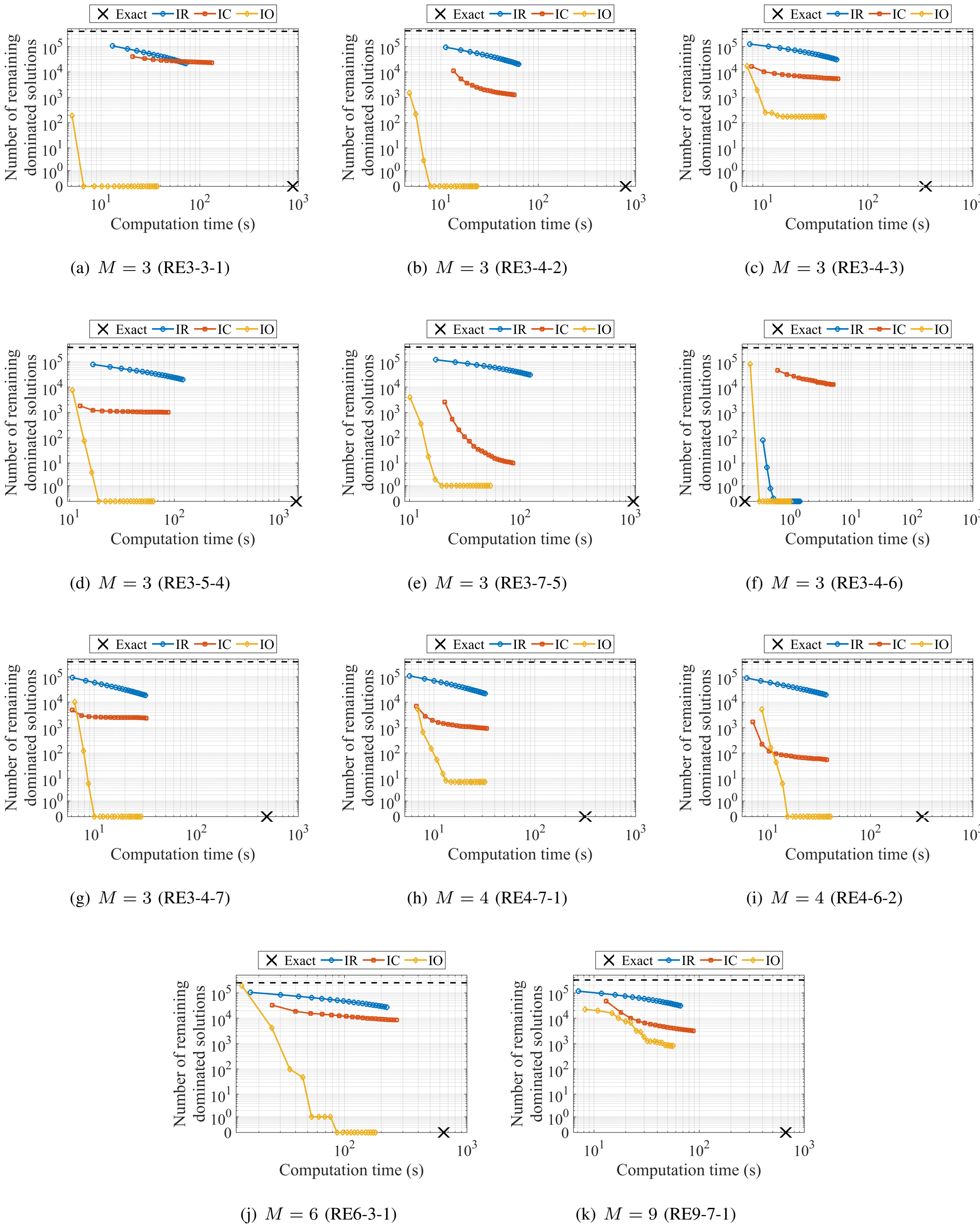

(a) $M = 3$ (RE3-3-1)

(b) $M = 3$ (RE3-4-2)

(c) $M = 3$ (RE3-4-3)

(d) $M = 3$ (RE3-5-4)

(e) $M = 3$ (RE3-7-5)

(f) $M = 3$ (RE3-4-6)

(g) $M = 3$ (RE3-4-7)

(h) $M = 4$ (RE4-7-1)

(i) $M = 4$ (RE4-6-2)

(j) $M = 6$ (RE6-3-1)

(k) $M = 9$ (RE9-7-1)

Fig. 5. Performance comparison of different methods for removing dominated solutions from the RE problems. Average values over ten runs are shown.

S2. Comparison between Hybrid Versions and Original Versions

Figure 6-8, Figure 9 and Figure 10 compare the hybrid partition methods and the original partition methods for the WFG, DTLZ and RE problems, respectively.

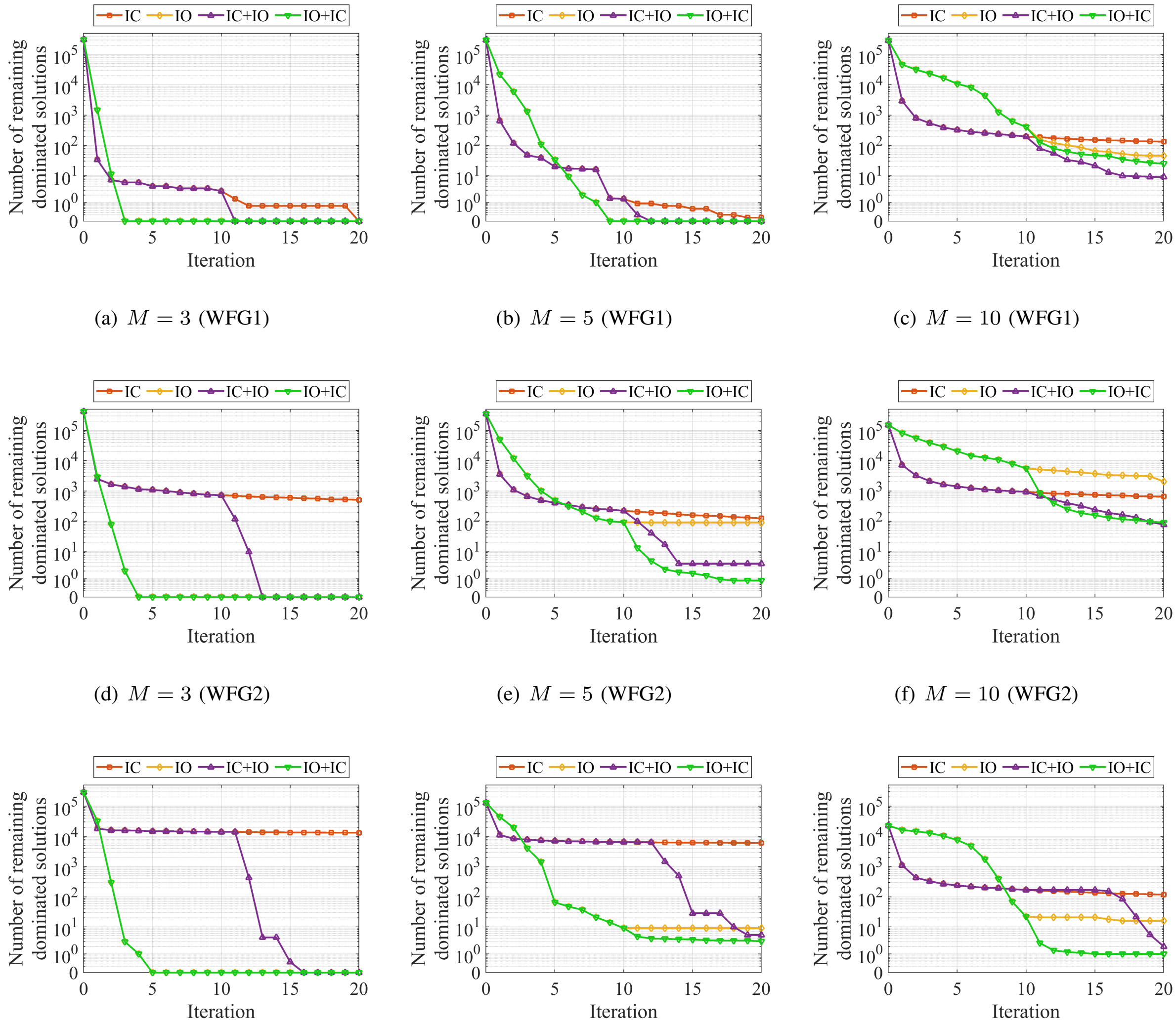

(a) $M = 3$ (WFG1) (b) $M = 5$ (WFG1) (c) $M = 10$ (WFG1)

(d) $M = 3$ (WFG2) (e) $M = 5$ (WFG2) (f) $M = 10$ (WFG2)

(g) $M = 3$ (WFG3) (h) $M = 5$ (WFG3) (i) $M = 10$ (WFG3)

Fig. 6. Comparison between the hybrid partition methods and the original partition methods for the WFG1-3 problems.

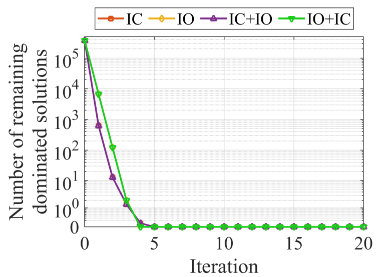

(a) $M = 3$ (WFG4)

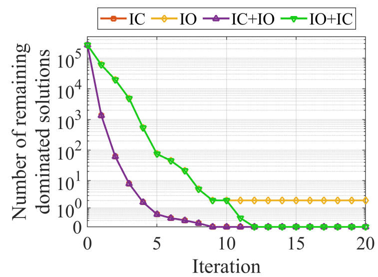

(b) $M = 5$ (WFG4)

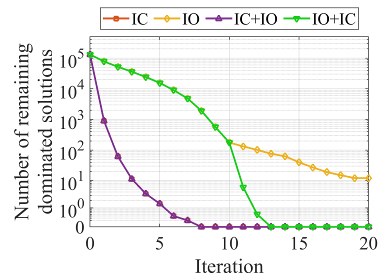

(c) $M = 10$ (WFG4)

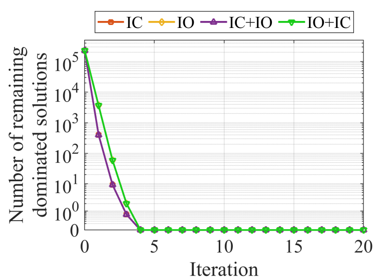

(d) $M = 3$ (WFG5)

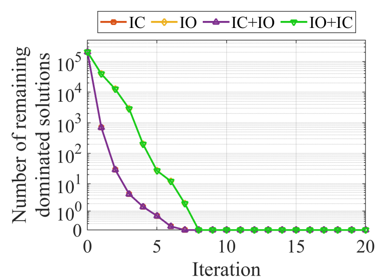

(e) $M = 5$ (WFG5)

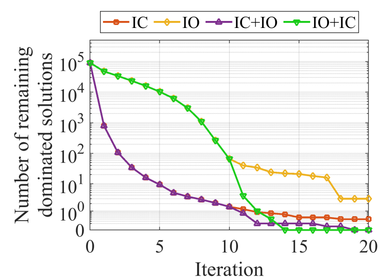

(f) $M = 10$ (WFG5)

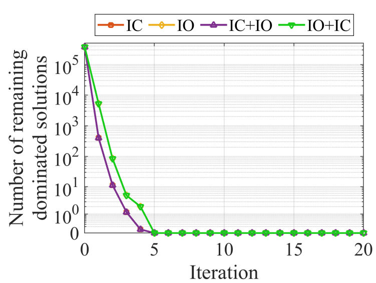

(g) $M = 3$ (WFG6)

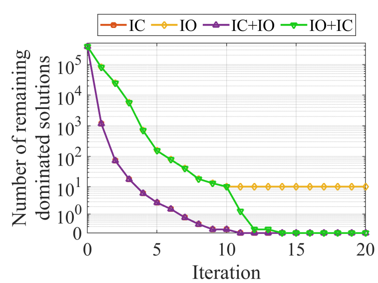

(h) $M = 5$ (WFG6)

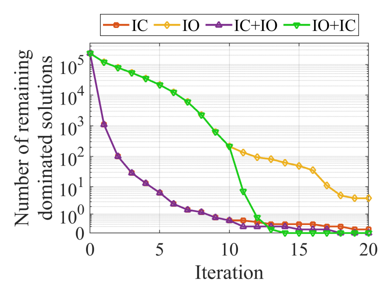

(i) $M = 10$ (WFG6)

Fig. 7. Comparison between the hybrid partition methods and the original partition methods for the WFG4-6 problems.

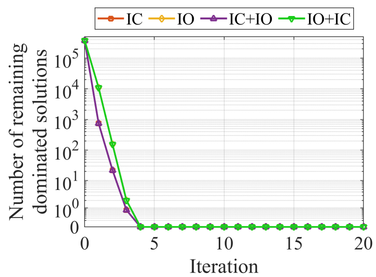

(a) $M = 3$ (WFG7)

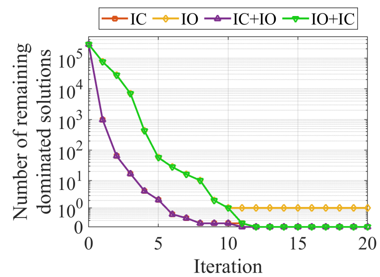

(b) $M = 5$ (WFG7)

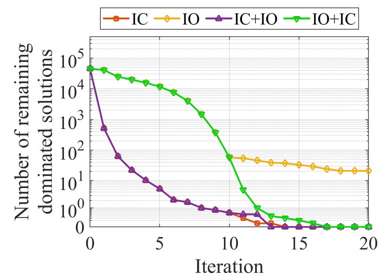

(c) $M = 10$ (WFG7)

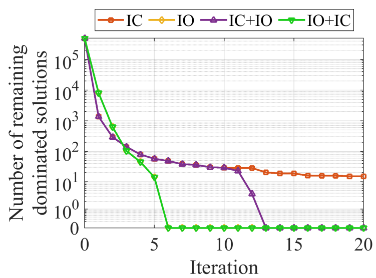

(d) $M = 3$ (WFG8)

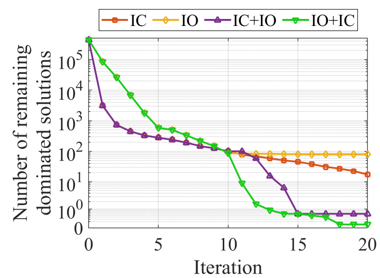

(e) $M = 5$ (WFG8)

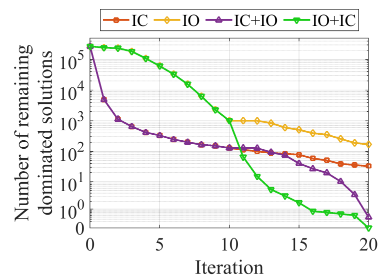

(f) $M = 10$ (WFG8)

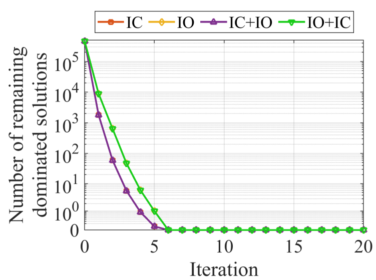

(g) $M = 3$ (WFG9)

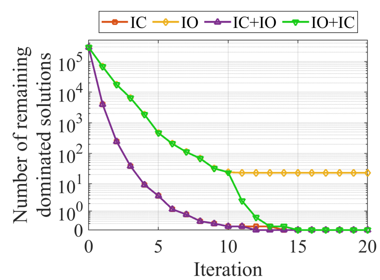

(h) $M = 5$ (WFG9)

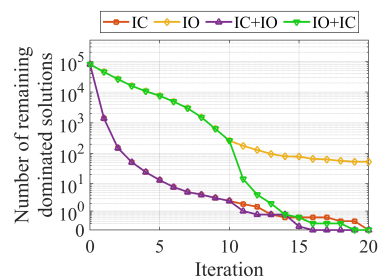

(i) $M = 10$ (WFG9)

Fig. 8. Comparison between the hybrid partition methods and the original partition methods for the WFG7-9 problems.

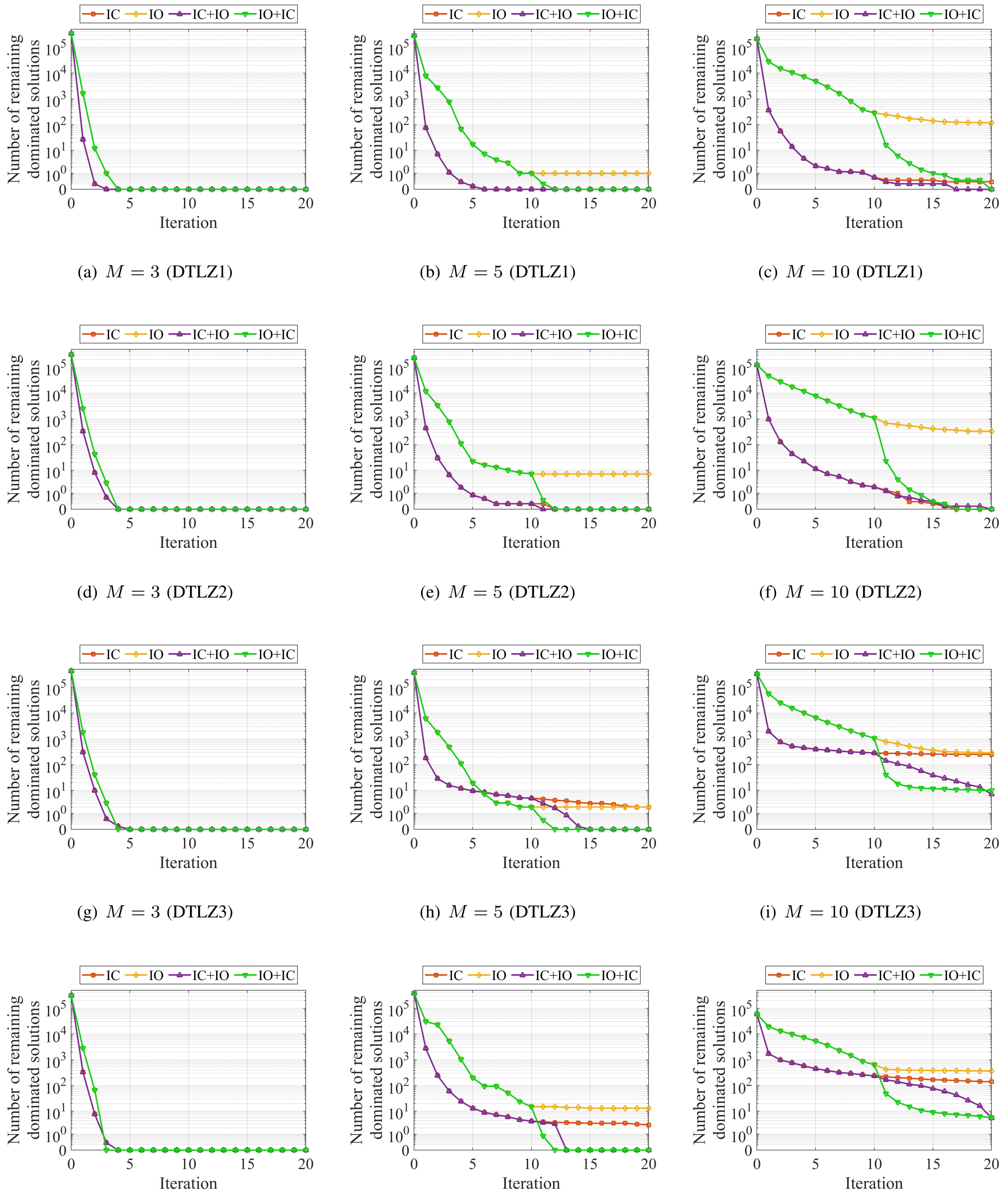

(a) $M = 3$ (DTLZ1) (b) $M = 5$ (DTLZ1) (c) $M = 10$ (DTLZ1)

(d) $M = 3$ (DTLZ2) (e) $M = 5$ (DTLZ2) (f) $M = 10$ (DTLZ2)

(g) $M = 3$ (DTLZ3) (h) $M = 5$ (DTLZ3) (i) $M = 10$ (DTLZ3)

(j) $M = 3$ (DTLZ4) (k) $M = 5$ (DTLZ4) (l) $M = 10$ (DTLZ4)

Fig. 9. Comparison between the hybrid partition methods and the original partition methods for the DTLZ1-4 problems.

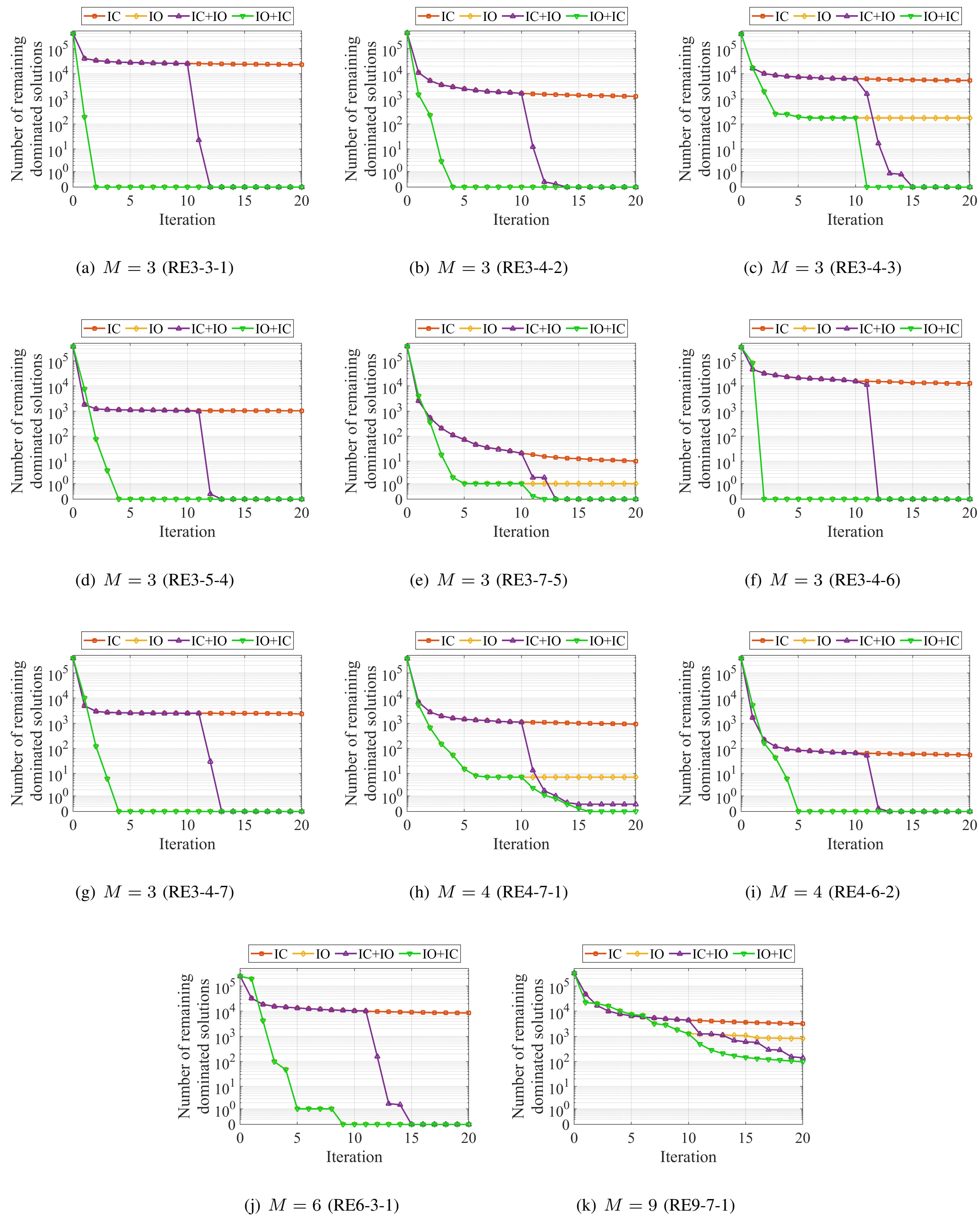

(a) $M = 3$ (RE3-3-1)

(b) $M = 3$ (RE3-4-2)

(c) $M = 3$ (RE3-4-3)

(d) $M = 3$ (RE3-5-4)

(e) $M = 3$ (RE3-7-5)

(f) $M = 3$ (RE3-4-6)

(g) $M = 3$ (RE3-4-7)

(h) $M = 4$ (RE4-7-1)

(i) $M = 4$ (RE4-6-2)

(j) $M = 6$ (RE6-3-1)

(k) $M = 9$ (RE9-7-1)

Fig. 10. Comparison between the hybrid partition methods and the original partition methods for the RE problems.

S3. Effects of the Number of Subsets for the Performance of Partition Methods

A. Computation Time

Figure 11-13, Figure 14 and Figure 15 show the effects of the number of subsets on the computation time of each partition method for the WFG, DTLZ and RE problems, respectively.

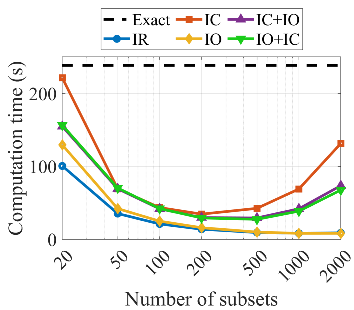

(a) $M = 3$ (WFG1)

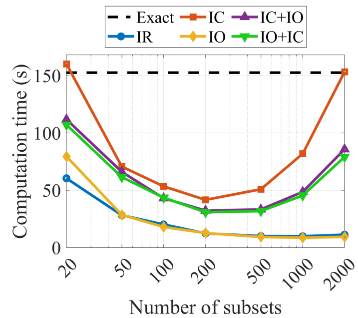

(b) $M = 5$ (WFG1)

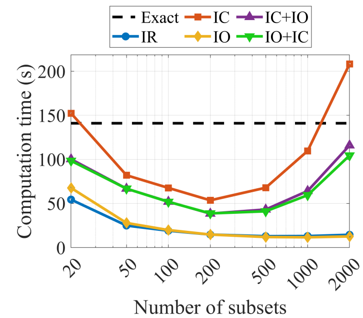

(c) $M = 10$ (WFG1)

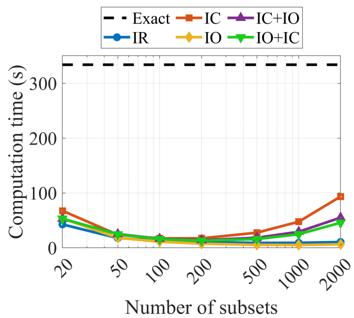

(d) $M = 3$ (WFG2)

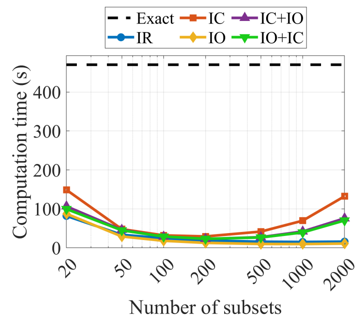

(e) $M = 5$ (WFG2)

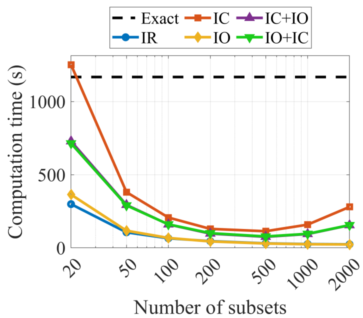

(f) $M = 10$ (WFG2)

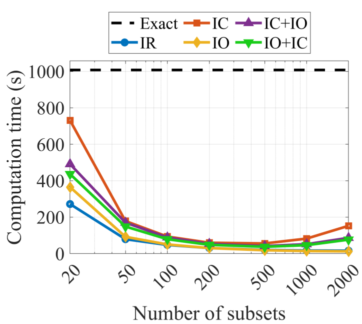

(g) $M = 3$ (WFG3)

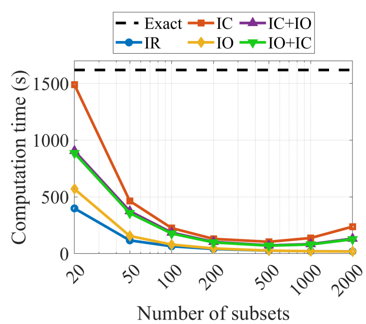

(h) $M = 5$ (WFG3)

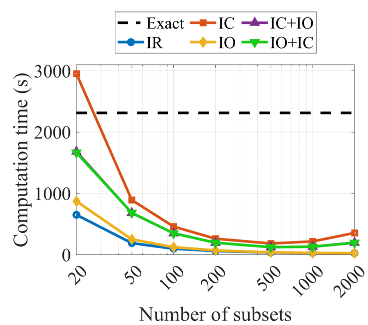

(i) $M = 10$ (WFG3)

Fig. 11. Computation time of each partition method with different specifications of the number of subsets for the WFG1-3 problems. The number of iterations is 20 in all partition methods. The dashed horizontal line shows the computation time of the exact method (where the number of subsets is one).

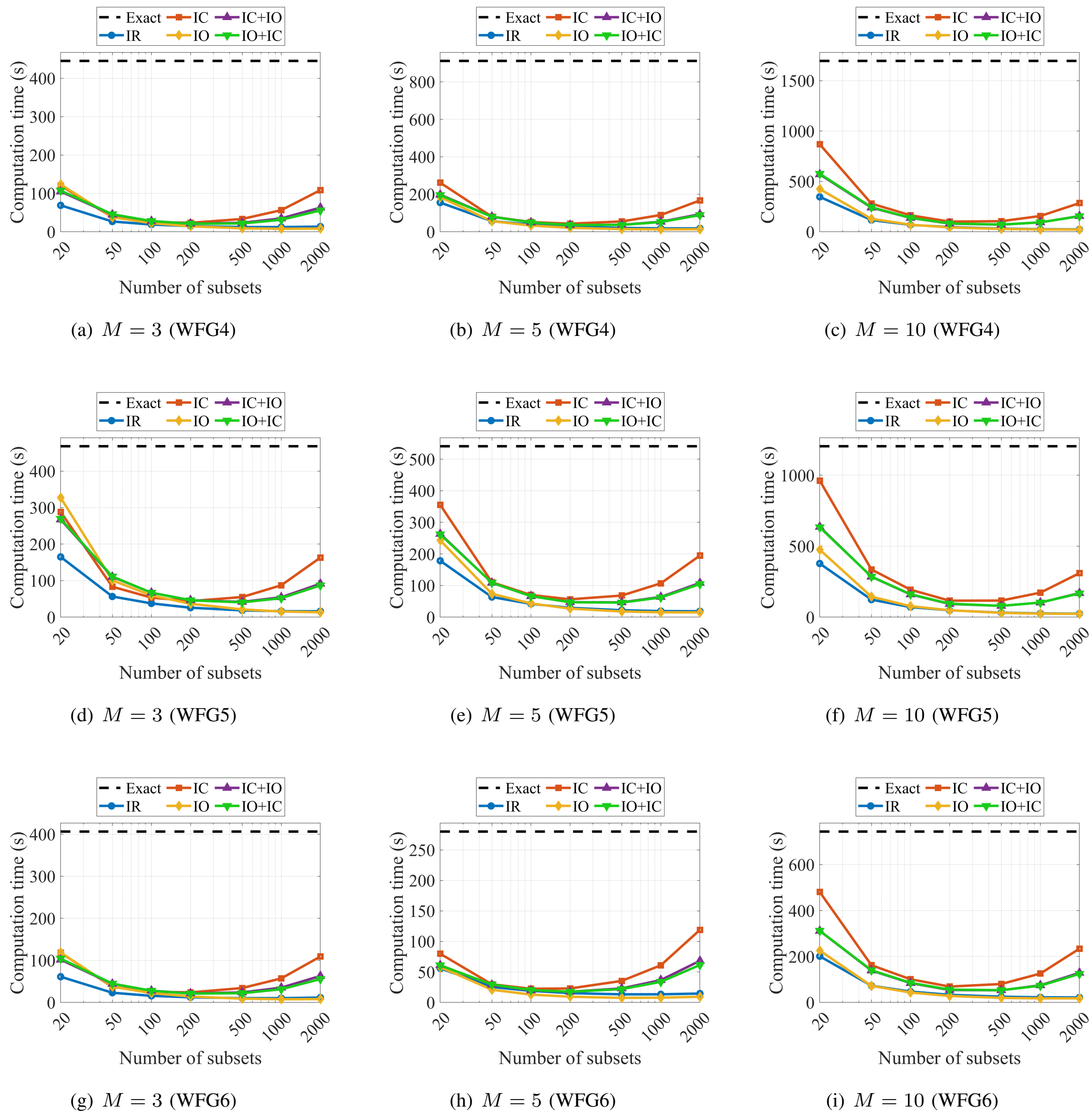

(a) $M = 3$ (WFG4) (b) $M = 5$ (WFG4) (c) $M = 10$ (WFG4)

(d) $M = 3$ (WFG5) (e) $M = 5$ (WFG5) (f) $M = 10$ (WFG5)

(g) $M = 3$ (WFG6) (h) $M = 5$ (WFG6) (i) $M = 10$ (WFG6)

Fig. 12. Computation time of each partition method with different specifications of the number of subsets for the WFG4-6 problems. The number of iterations is 20 in all partition methods. The dashed horizontal line shows the computation time of the exact method (where the number of subsets is one).

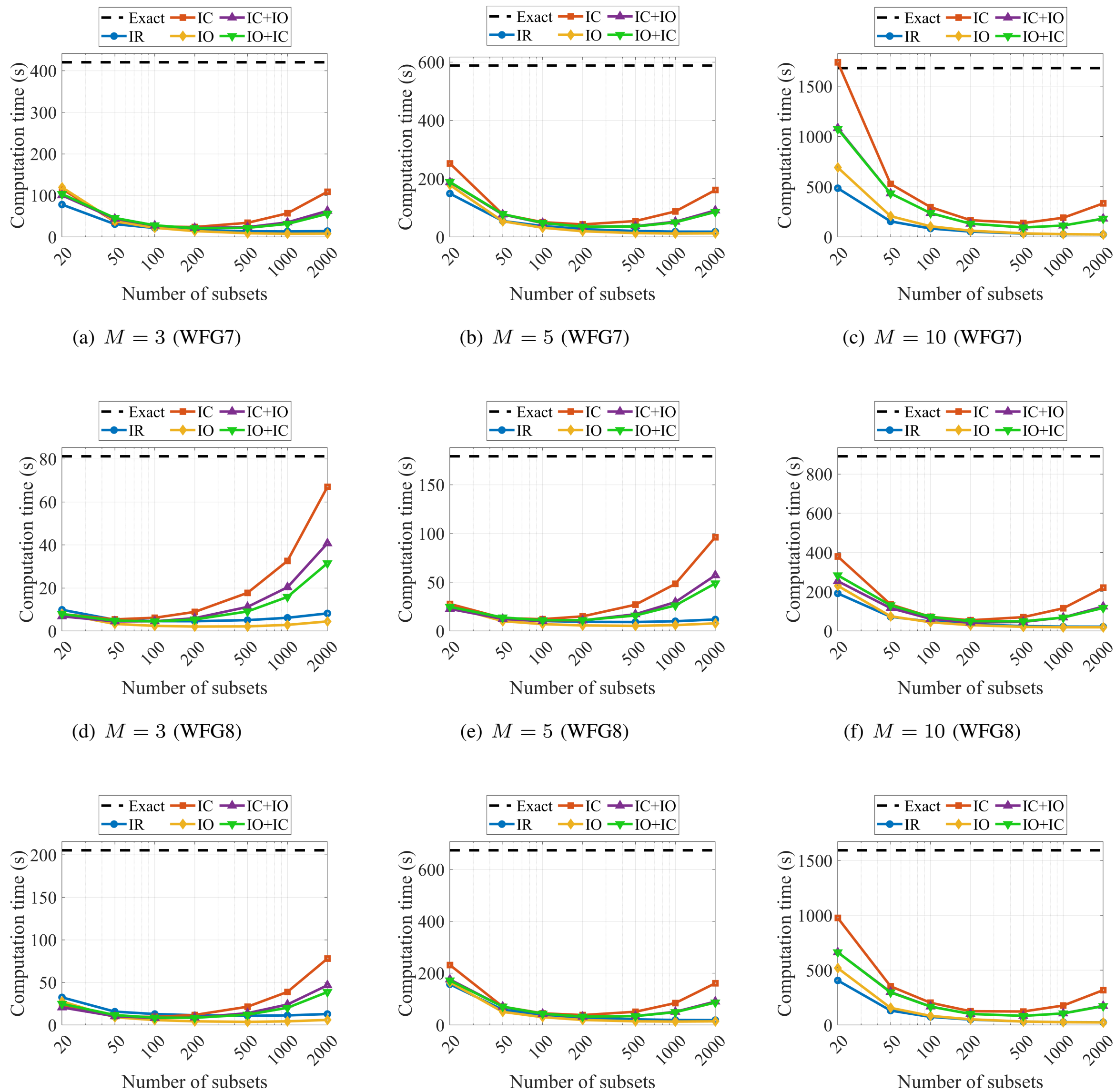

(a) $M = 3$ (WFG7)
(b) $M = 5$ (WFG7)
(c) $M = 10$ (WFG7)
(d) $M = 3$ (WFG8)
(e) $M = 5$ (WFG8)
(f) $M = 10$ (WFG8)
(g) $M = 3$ (WFG9)
(h) $M = 5$ (WFG9)
(i) $M = 10$ (WFG9)

Fig. 13. Computation time of each partition method with different specifications of the number of subsets for the WFG7-9 problems. The number of iterations is 20 in all partition methods. The dashed horizontal line shows the computation time of the exact method (where the number of subsets is one).

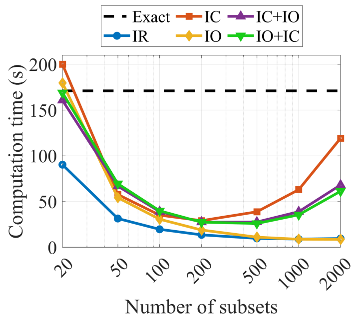

(a) $M = 3$ (DTLZ1)

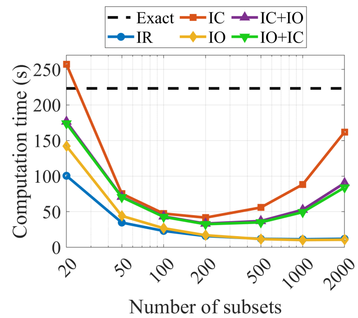

(b) $M = 5$ (DTLZ1)

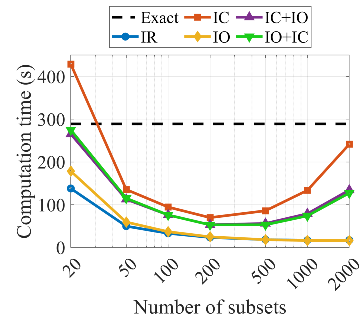

(c) $M = 10$ (DTLZ1)

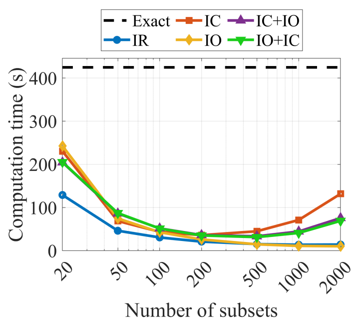

(d) $M = 3$ (DTLZ2)

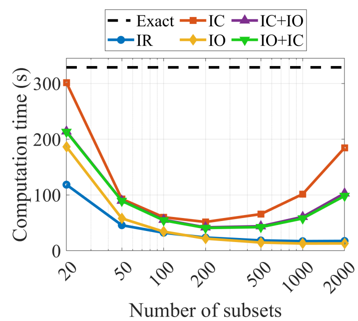

(e) $M = 5$ (DTLZ2)

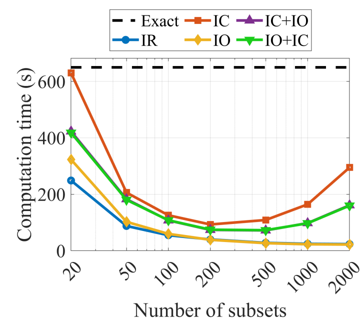

(f) $M = 10$ (DTLZ2)

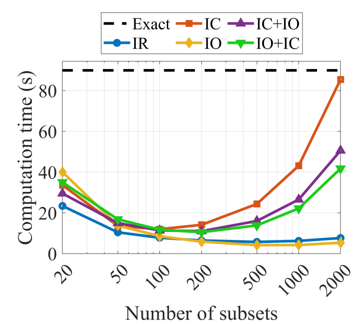

(g) $M = 3$ (DTLZ3)

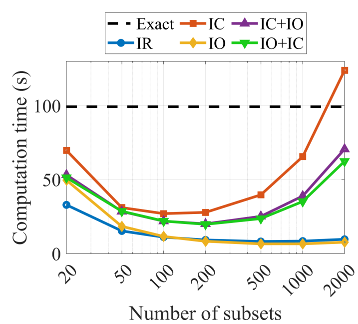

(h) $M = 5$ (DTLZ3)

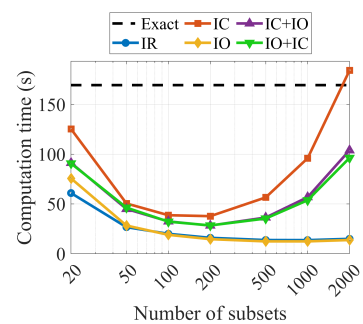

(i) $M = 10$ (DTLZ3)

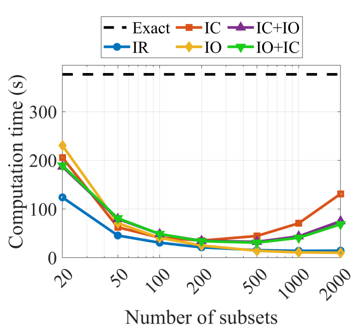

(j) $M = 3$ (DTLZ4)

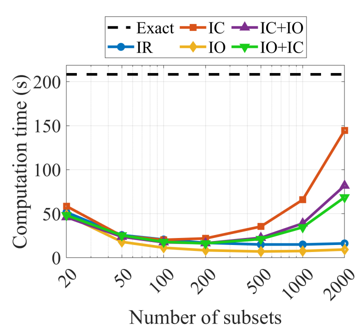

(k) $M = 5$ (DTLZ4)

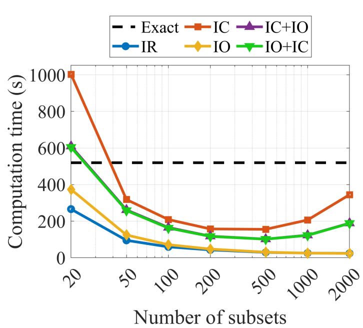

(l) $M = 10$ (DTLZ4)

Fig. 14. Computation time of each partition method with different specifications of the number of subsets for the DTLZ1-4 problems. The number of iterations is 20 in all partition methods. The dashed horizontal line shows the computation time of the exact method (where the number of subsets is one).

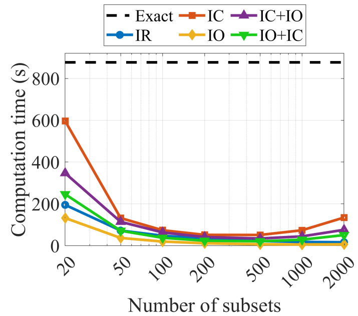

(a) $M = 3$ (RE3-3-1)

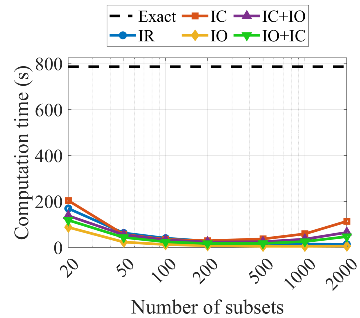

(b) $M = 3$ (RE3-4-2)

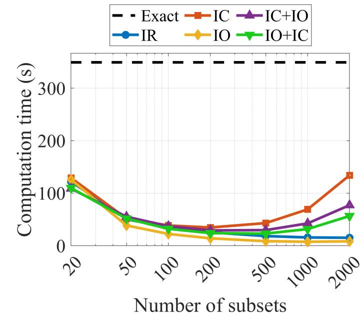

(c) $M = 3$ (RE3-4-3)

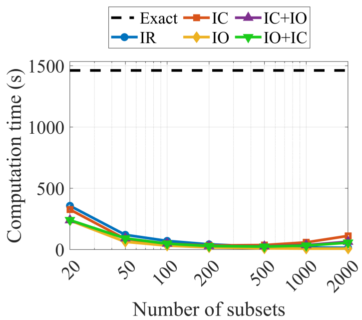

(d) $M = 3$ (RE3-5-4)

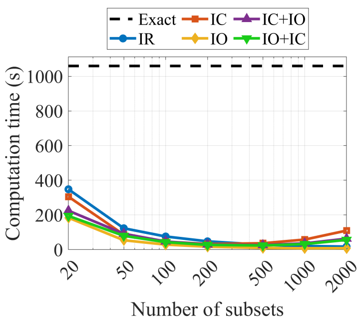

(e) $M = 3$ (RE3-7-5)

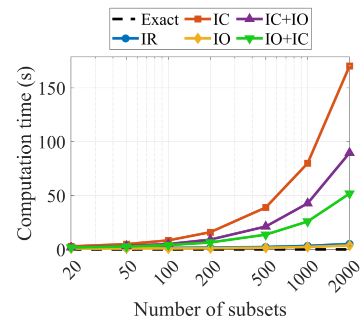

(f) $M = 3$ (RE3-4-6)

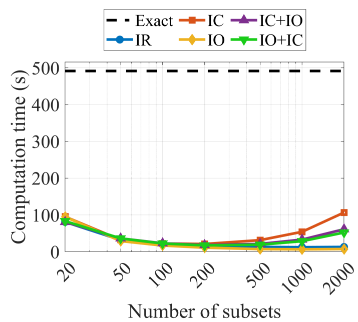

(g) $M = 3$ (RE3-4-7)

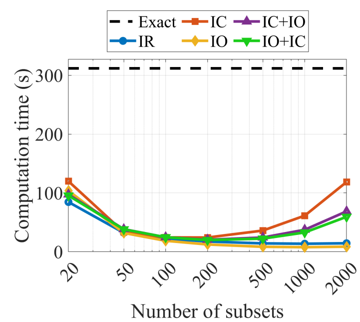

(h) $M = 4$ (RE4-7-1)

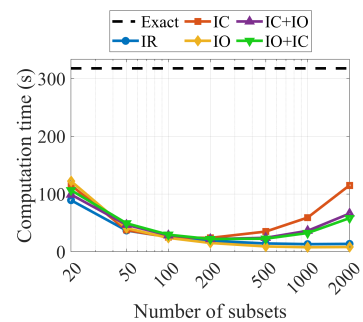

(i) $M = 4$ (RE4-6-2)

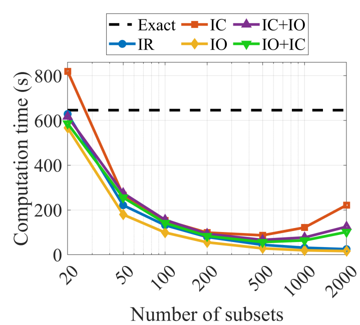

(j) $M = 6$ (RE6-3-1)

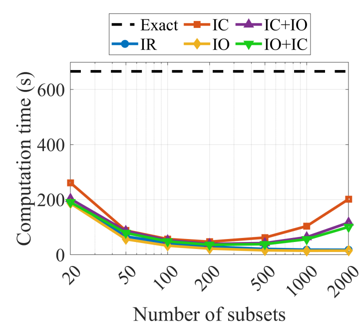

(k) $M = 9$ (RE9-7-1)

Fig. 15. Computation time of each partition method with different specifications of the number of subsets for the RE problems. The number of iterations is 20 in all partition methods. The dashed horizontal line shows the computation time of the exact method (where the number of subsets is one).

B. Number of Remaining Dominated Solutions

Figure 16-18, Figure 19 and Figure 20 show the effects of the number of subsets on the removal performance (i.e., the number of remaining dominated solutions) of each partition method for the WFG, DTLZ and RE problems, respectively.

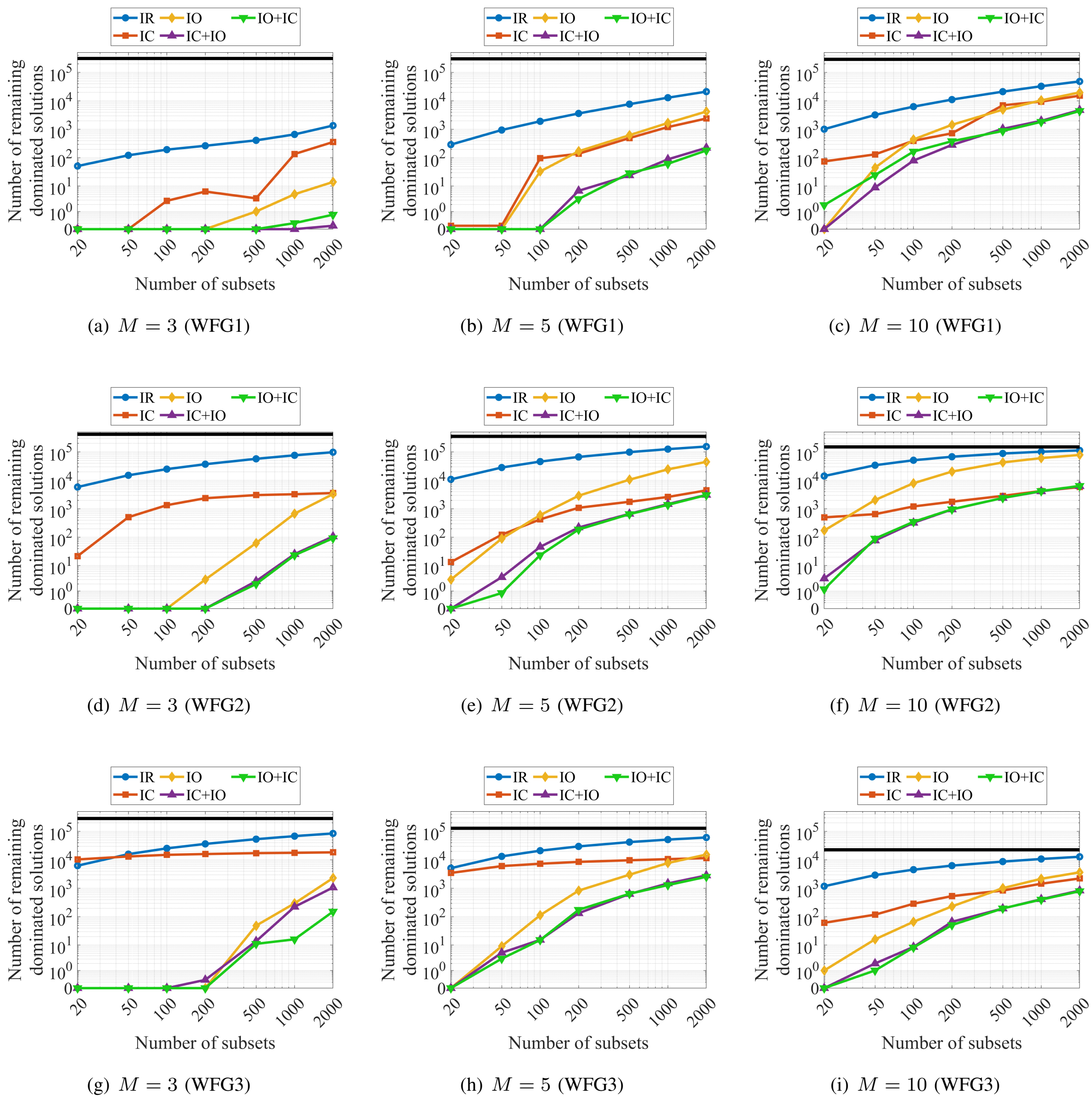

(a) $M = 3$ (WFG1) (b) $M = 5$ (WFG1) (c) $M = 10$ (WFG1)

(d) $M = 3$ (WFG2) (e) $M = 5$ (WFG2) (f) $M = 10$ (WFG2)

(g) $M = 3$ (WFG3) (h) $M = 5$ (WFG3) (i) $M = 10$ (WFG3)

Fig. 16. Number of remaining dominated solutions by each partition method with different specifications of the number of subsets for the WFG1-3 problems. The bold horizontal line shows the number of dominated solutions included in each solution set with 500,000 solutions.

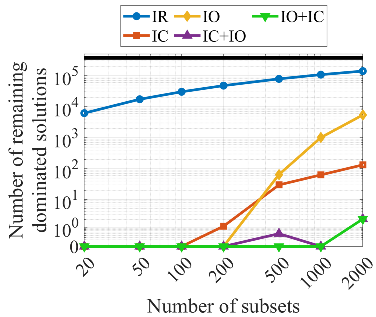

(a) $M = 3$ (WFG4)

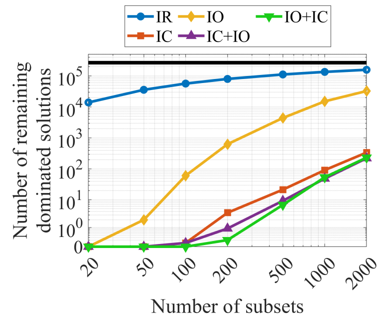

(b) $M = 5$ (WFG4)

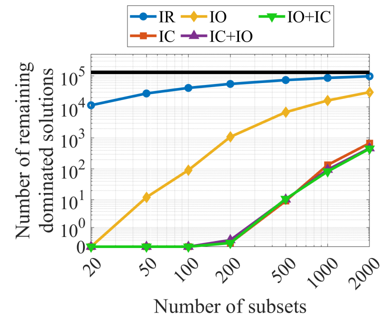

(c) $M = 10$ (WFG4)

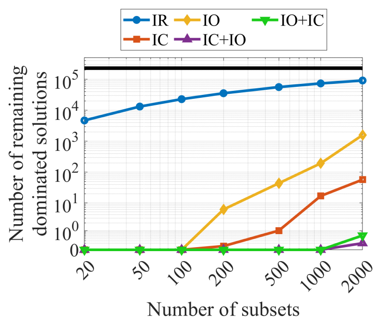

(d) $M = 3$ (WFG5)

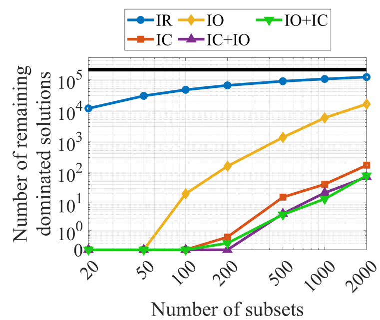

(e) $M = 5$ (WFG5)

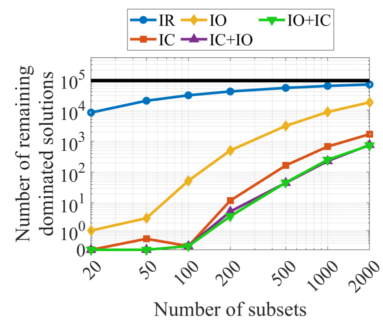

(f) $M = 10$ (WFG5)

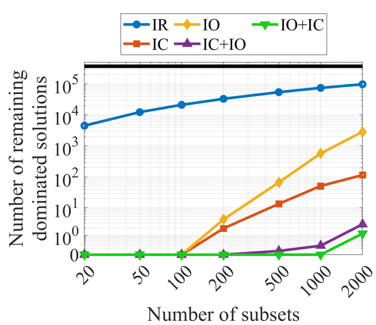

(g) $M = 3$ (WFG6)

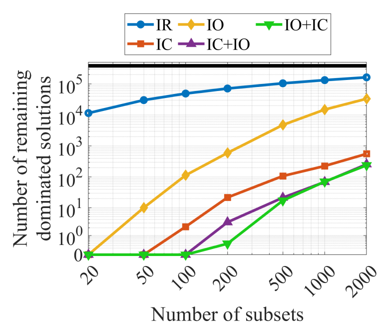

(h) $M = 5$ (WFG6)

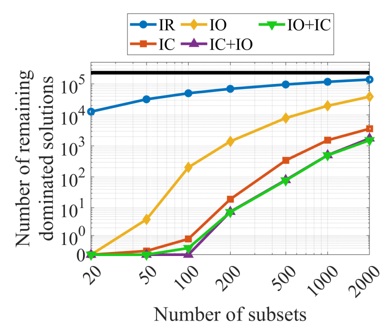

(i) $M = 10$ (WFG6)

Fig. 17. Number of remaining dominated solutions by each partition method with different specifications of the number of subsets for the WFG4-6 problems. The bold horizontal line shows the number of dominated solutions included in each solution set with 500,000 solutions.

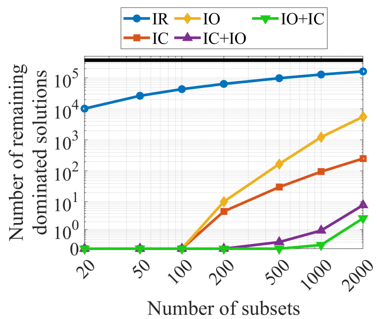

(a) $M = 3$ (WFG7)

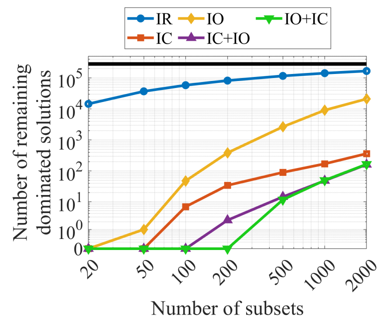

(b) $M = 5$ (WFG7)

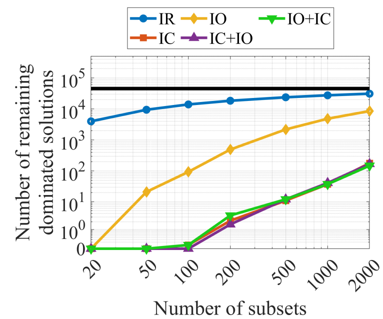

(c) $M = 10$ (WFG7)

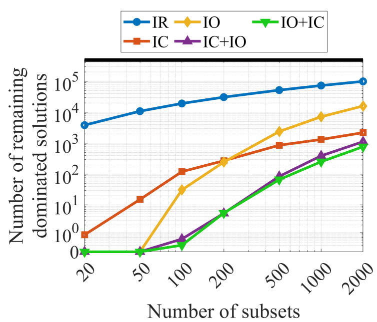

(d) $M = 3$ (WFG8)

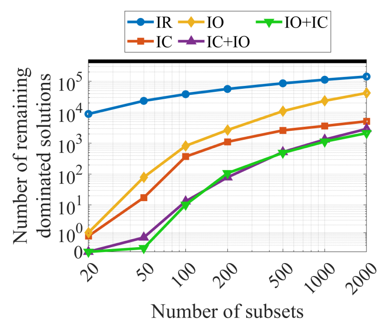

(e) $M = 5$ (WFG8)

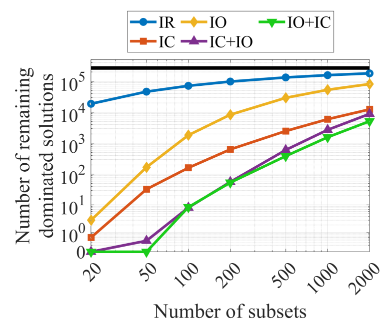

(f) $M = 10$ (WFG8)

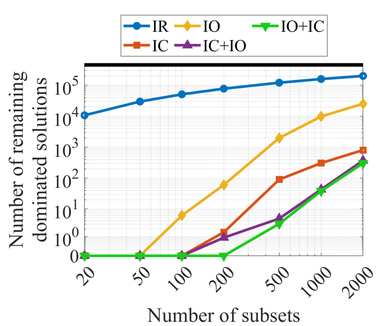

(g) $M = 3$ (WFG9)

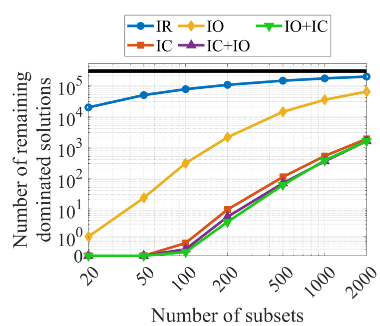

(h) $M = 5$ (WFG9)

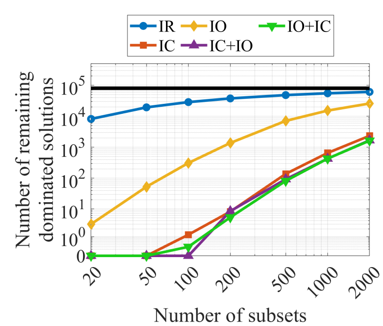

(i) $M = 10$ (WFG9)

Fig. 18. Number of remaining dominated solutions by each partition method with different specifications of the number of subsets for the WFG7-9 problems. The bold horizontal line shows the number of dominated solutions included in each solution set with 500,000 solutions.

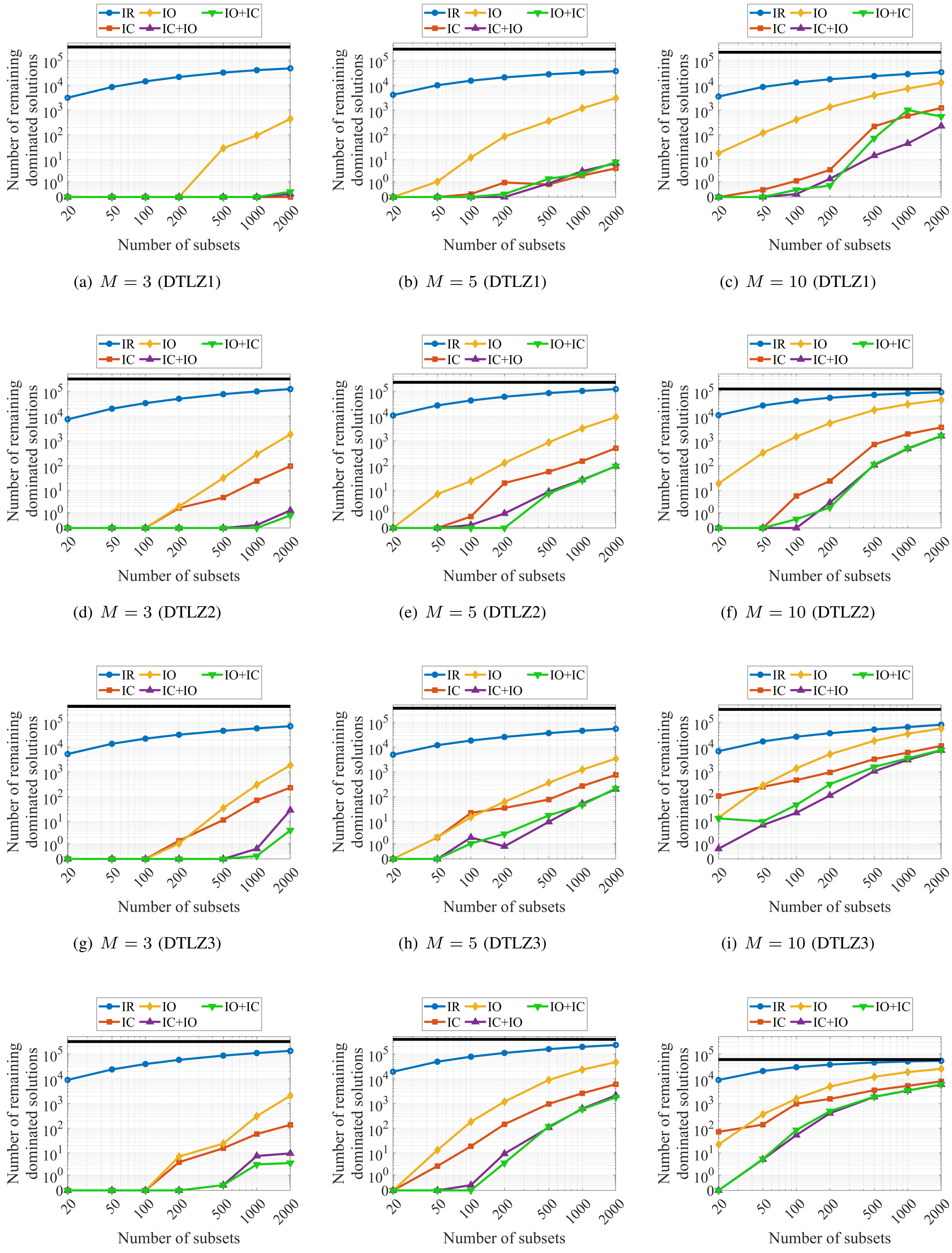

(a) $M = 3$ (DTLZ1) (b) $M = 5$ (DTLZ1) (c) $M = 10$ (DTLZ1)

(d) $M = 3$ (DTLZ2) (e) $M = 5$ (DTLZ2) (f) $M = 10$ (DTLZ2)

(g) $M = 3$ (DTLZ3) (h) $M = 5$ (DTLZ3) (i) $M = 10$ (DTLZ3)

(j) $M = 3$ (DTLZ4) (k) $M = 5$ (DTLZ4) (l) $M = 10$ (DTLZ4)

Fig. 19. Number of remaining dominated solutions by each partition method with different specifications of the number of subsets for the DTLZ1-4 problems. The bold horizontal line shows the number of dominated solutions included in each solution set with 500,000 solutions.

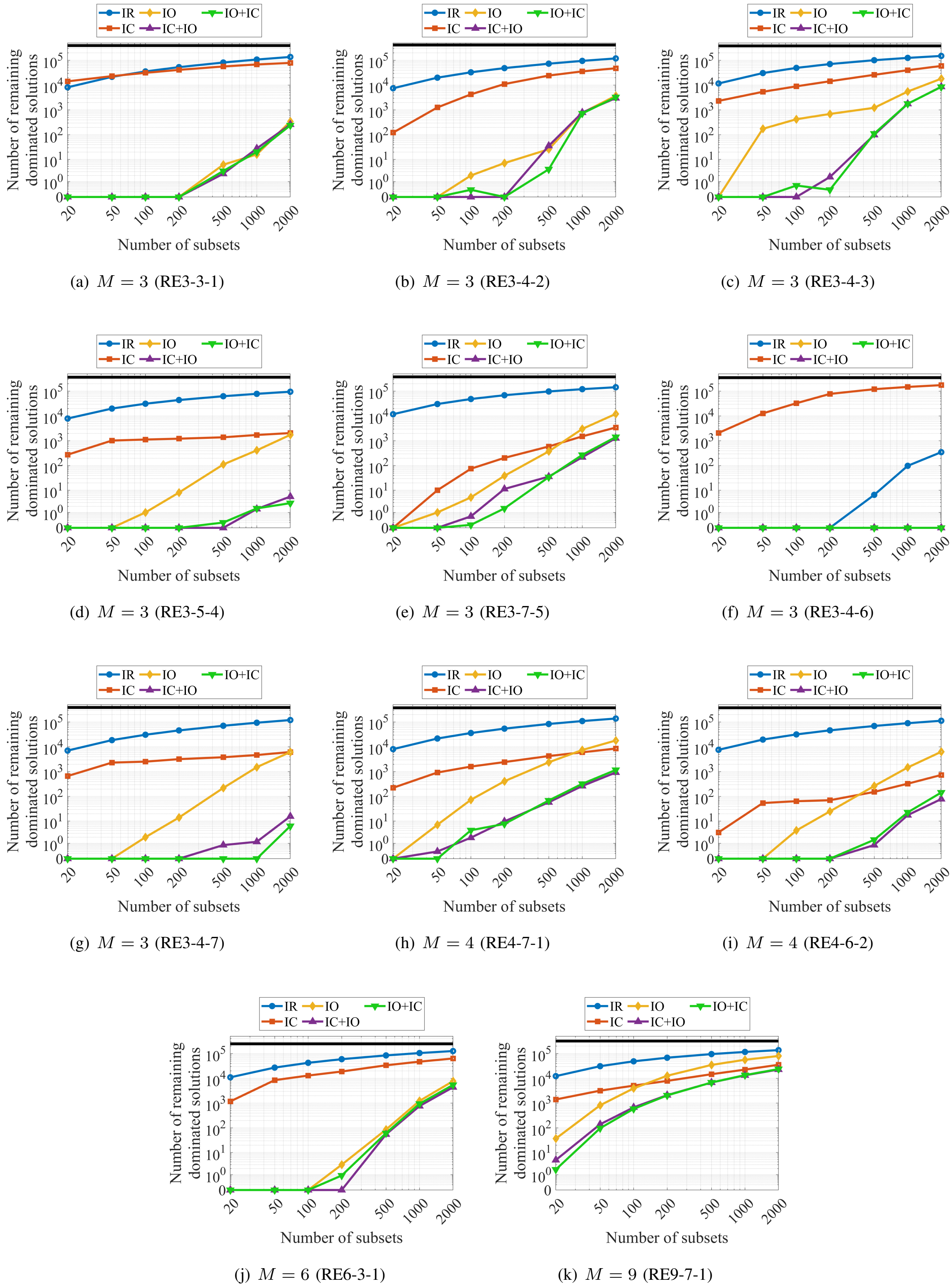

(a) $M = 3$ (RE3-3-1)
(b) $M = 3$ (RE3-4-2)
(c) $M = 3$ (RE3-4-3)
(d) $M = 3$ (RE3-5-4)
(e) $M = 3$ (RE3-7-5)
(f) $M = 3$ (RE3-4-6)
(g) $M = 3$ (RE3-4-7)
(h) $M = 4$ (RE4-7-1)
(i) $M = 4$ (RE4-6-2)
(j) $M = 6$ (RE6-3-1)
(k) $M = 9$ (RE9-7-1)

Fig. 20. Number of remaining dominated solutions by each partition method with different specifications of the number of subsets for the RE problems. The bold horizontal line shows the number of dominated solutions included in each solution set with 500,000 solutions.

S4. Effects of the Solution Distribution

The dominated solutions and their corresponding dominating solutions have both small cosine similarity-based difference and small objective value-based difference in the 3-objective DTLZ2 problem as shown in Figure 7 (a) of the paper. This is because the DTLZ2 problem has a regular shape Pareto front and a regular shape feasible region as shown in Figure 21 (a). The WFG4 problem also has a regular Pareto front and a regular feasible region as shown in Figure 21 (b). This explains why very similar results were obtained for the DTLZ2 and WFG4 problems in the paper.

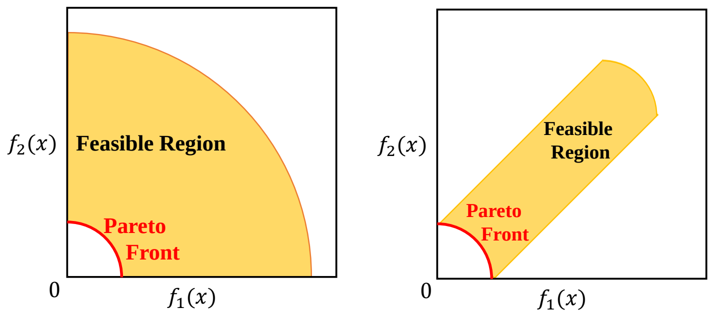

(a) DTLZ2-4 (b) WFG4-9

Fig. 21. An illustration of the Pareto front and the feasible region of two-objective DTLZ2-4 and WFG 4-9 problems.

For the RE3-3-1 problem, each dominated solution has large cosine similarity-based difference while it has small objective similarity-based difference as shown in Figure 7 (b) of the paper. This observation means that cosine similarity is less useful to group the dominated solutions and their corresponding dominating solutions for the RE3-3-1 problem. In Figure 22 (a), we plot 50 subsets at the 20th iteration of the cosine similarity-based partition method for the RE3-3-1 problem. As we can see all, each objective has a totally different range. After carefully examinations of all solutions, we found that all each solution has a small f_1 value (i.e., $f_1 < 13$) or a small f_2 value (i.e., $f_2 < 13$). However, their f_3 values vary from 0 to 2×10^7. That is, all solutions are close to the $f_2 - f_3$ plane with $f_1 = 0$ or the $f_1 - f_3$ plane with $f_2 = 0$. Figure 22 (b) focuses on the subspace of the objective space with $0 \leq f_2 \leq 13$. In Figure 22 (b), we show a dominated solution and its single corresponding dominating solution. These two solutions have similar f_1 and f_2 values, but different f_3 values. Thus, this dominated solution is not grouped together with its dominating solution in the same subset, and not removed by the cosine similarity-based partition method. There are 14,770 such remaining dominated solutions in Figure 22 (b). This explains why the cosine similarity-based partition method shows poor performance whereas the objective value-based partition method works well for the RE3-3-1 problem.

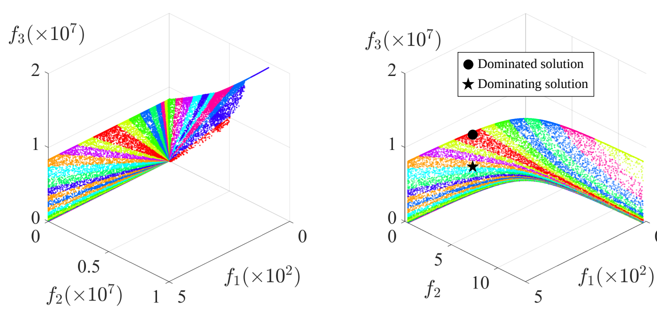

(a) (b)

Fig. 22. (a) Plot of 50 subsets obtained by the cosine similarity-based partition method at the 20-th iteration for the RE3-3-1 problem. (b) A focused plot into the range of $[0, 13]$ of the f_2 values whereas the range of the f_2 values in (a) is $[0, 10^7]$.